Proceedings of the 2013 International Symposium on Liquid Metal Processing & Casting
Edited by: Matthew J. M. Krane, Alain Jardy, Rodney L. Williamson, and Joseph J. Beaman
TMS (The Minerals, Metals & Materials Society), 2013

INCLUSION BEHAVIOR IN STEEL AND ALUMINUM MAKING REACTORS

J.P. Bellot, O. Mirgaux, A. Jardy
Institut Jean Lamour, UMR 7198, CNRS ('LabEx DAMAS')/ Université de Lorraine, F-54011 Nancy, France
Key words: Inclusion, steel, aluminum, ladle, simulation, population balance

Abstract

The control of inclusion population remains an important issue for the steelmaking and aluminum making industries where the removal of particles is mainly operated by flotation and gravity separation. Argon gas is injected through porous plugs in the ladle of liquid steel whereas a rotating impeller and a mixture of argon and chlorine stir up the aluminum liquid bath. Nowadays the modeling of such complex three-phase-reactors is possible by combining Population Balance with convective transport of the inclusions so as to calculate the time evolution of the size distribution of the inclusion population. An operator splitting technique is employed to solve the coupled Population Balance Equation and the transport equation. Results are provided for either pilot or industrial scales and allow us to compare the respective roles of mechanisms (flotation, entrapment on the liquid surface, gravity separation, agglomeration) on the particle size distribution and on the inclusion removal rate.

Introduction

The control of metal cleanliness has always been an issue of great concern for the metallurgists since the inclusions influence directly the mechanical properties of the alloys mainly the workability, surface quality and fatigue strength. In most of the metallurgical routes a refining treatment of the molten alloy has been introduced in particular with the aim of improving the metal cleanliness which means a better control of the amount, the size and morphology and finally the composition of inclusions. After solidification of the metal these properties can be quantified by either destructive or non-destructive assessment techniques but the cleanliness can be hardly modified by thermal treatments. That is one very good reason why the inclusion treatment occurs before casting. Since the beginning of the XXIst century this issue is a new challenge for the metallurgists for two main reasons: on one hand the reduction in the weight of high performance materials together with the improvement of mechanical properties requires an improvement of the metal cleanliness. On the other hand the increase of the recycling of used metal reinforces the role of molten metal refining. Gas-stirring ladle treatment of liquid metal has been pointed out for a long time as the processing stage mainly responsible for the inclusion population of aluminum and specialty steels. A particular attention has been paid on the optimization of this complex three-phase-reactor, where strongly dispersed inclusions are transported by the turbulent liquid metal / bubbles flow.

The numerical simulation of such complex metallurgical reactor has already been the purpose of many studies. The mathematical modeling became in the early '70s an intrinsic part of materials engineering and the numerical simulation of refining reactors has been initially driven by Szekely. Hence as an example, Nakamishi and Szekely [1] initiate the use of k-ε turbulent model for the prediction of agglomeration kernels in order to estimate the Al deoxidation rate of liquid steel reactor. Other authors followed this approach among them Guthrie [2,3] who improved step by step the numerical simulation of gas stirred ladle systems. Mazundar and Guthrie published in 1995 a relatively exhaustive review addressing physical and mathematical models of ladles. Since then, the simulations of liquid metal processing were developed with an increasing level of sophistication. This type of work, performed under the leadership of KTH in Stockholm [4] and the University of Urbana-Champaign [5], can be considered as a benchmark in this field. KTH and Mefos in Sweden have carried out a number of projects within Jernkontoret'research especially focused on non-metallic inclusions in ladle and tundish. Jonsson [6] pointed out that the understanding of particle behavior nearby the liquid surface remains very poor and no model exists for predicting the deposition rate. The authors gave a first approach by Lagrangian calculation of particles near the slag-liquid interface and concluded on the role of particle inertia on the deposition rate. A similar approach has been followed by Gardin [7] revealing a lack of a detailed description of the non-isotropic and damped turbulence near the interface.

An integrated model coupling CFD and a nucleation-growth-removal model has been recently developed in Postech by Kwon et al. [8]. Even if the authors do not provide all the details of the numerical methods employed the numerical platform is probably one of the most integrated since in addition to the bubble-liquid flow calculated by an Eulerian-Lagrangian method the model simulates nucleation, growth and agglomeration of inclusions. Recently, a very innovative work was performed by Claudotte et al. [9] by coupling a population balance equation (PBE) with the computational fluid dynamics (CFD) to model the convective transport of particles and the probability of collisions due to the turbulent molten steel flow and the changes of particle properties due to breakup and aggregation. A variant of the quadrature method of moments (QMOM) has been adapted by the authors for the prediction of inclusion population in terms of chemical composition and size taken into consideration nucleation, diffusion growth and aggregation. A comparison of two numerical methods for solving the PBE is given by Daoud et al. [10] and reveals that the QMOM and the CM (class method) lead to similar results. However, most models used by these authors should be regarded as general models of processes that do not accurately describe the behavior and the capture of particles at interfaces (refractory wall, surface and bubbles).

In this paper we present the development, using the CFD code as a basis, of two- or three-dimensional simulation models applied to aluminum and steel stirred reactors.

The metallurgical reactors

Liquid metal processing shows similarities between aluminum and steel since in both cases the argon injection is operated. Flotation is one of the aims of gas injection which is a process widely used in industry to separate particles from a continuous liquid phase. During their ascension through the bulk, the bubbles collect the dispersed particles and release them at the surface, where they accumulate in the dross layer for Al and in the slag for

steel. Figures 1a and 1b give a schematic diagram of the ladles used in the two industries. In the Al flotation tank, the gas (often a mixture of chlorine and argon) is injected into the melt through a rotating impeller. This impeller generates a turbulent fluid flow in the reactor, enhancing the probability of collisions between bubbles and unwanted inclusions. In the steel ladle , an injection of argon through one or more porous plugs at the bottom of the reactor provides both mixing of the liquid metal to achieve thermal and chemical homogeneity and the entrapment of the inclusions by the flotation mechanism.

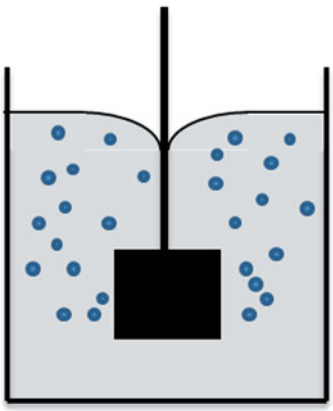

Figure 1a: Al flotation tank

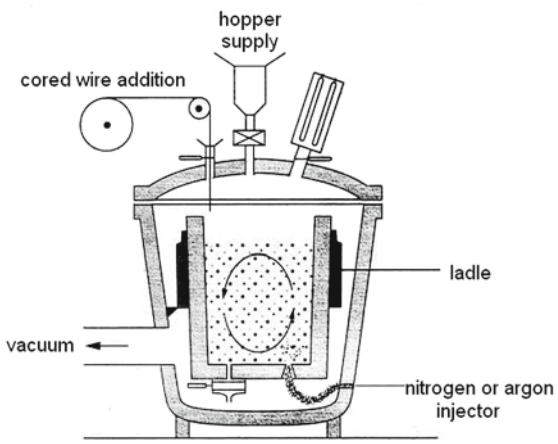

Figure 1b: Steel gas stirred ladle

Inclusions most frequently found in molten aluminum are oxide films, refractory particles and aluminum carbide (originating from refractory degradation or refractory metal reactions). Inclusion population in molten steel is mainly composed of non-metallic oxide inclusions such as calcium aluminate inclusions. Size of these inclusions may vary from one micrometer to a few hundreds micrometers, for the coarsest ones.

Hence, the technology applied to remove the inclusions remains quite similar. The mechanisms involved are:

- the collisions between inclusions, which can lead to aggregation and even to agglomeration if reconstruction of the aggregate occurs,
- the collisions with bubbles, which lead to the mechanism of flotation,
- the entrapment at the interface between the liquid bath and slag coverage,
- the separation induced by gravity.
- the entrapment at the ladle walls.

Mathematical modeling

The approach adopted for reactor modeling is divided into two parts. The bubbles plume play an important role in metal bath mixing while, owing to their small weight fraction (<0.01%), the inclusions do not affect the flow. First, the two-phase flow turbulent bubble-liquid metal is simulated for the 2D or 3D geometry of the ladle and a strong coupling is achieved between the liquid metal and the bubbles. This resolution provides the velocity fields as well as the maps of local flow turbulence and retention rate (gas volume fraction in the mixture); these data define the conditions of inclusion interaction (aggregation, flotation, entrapment). Details of the hydrodynamic modeling will be found in ref. [11]. In the second step, the behavior of the inclusion population is caused to both the transport at the macroscopic scale of the ladle and the interaction mechanisms at the mesoscopic scale of the particle. The main features of this mathematical modeling are presented below.

As presented by Kumar and Ramkrishna [12], population balance is a powerful way of synthesizing the behavior of a population of discrete particles from the behavior of single particles in their local environment. The behavior of the inclusion population, defined by a distribution function of particle size (N_i is the number of inclusions of class "i" –volume of the particle is between v_i and v_{i+1} -per m^3 of liquid metal), is described by the population balance equation (PBE). Equation (4) represents the macroscopic transport phenomena of inclusions (left member), and mesoscopic phenomena such as bubble-inclusion (flotation Z_{bi}) and inclusion-inclusion (aggregation B_i-D_i) interactions:

$$\frac{\partial \alpha_l N_i}{\partial t} + div(\alpha_l \mathbf{u}_l N_i) = \alpha_l \left(B_i - D_i\right) - \alpha_l Z_{bi} - S_i \quad (1)$$

In equation (4), S_i is the inclusion gravity separation term.

The transient solution to this equation can be obtained by separating the transport and collision operators [13]. In the first step, the transport equation of the quantity N_i is solved using the Finite Volume Method:

$$\frac{\partial \alpha_l N_i}{\partial t} + div(\alpha_l \boldsymbol{u}_l N_i) = 0 \quad (2)$$

In the second step, the population balance (equation 6) is solved in each control volume applying the cell average technique [14] which is a variant of the fixed pivot method of Kumar and Ramkrishna [12] leading to a significant reduction in numerical diffusion:

$$\frac{\partial \alpha_l N_i}{\partial t} = \alpha_l \left(B_i - D_i\right) - \alpha_l Z_{bi} - S_i \quad (3)$$

The aggregation and flotation kernels are an issue of great development and the reader will find details of the physical phenomena and of the applied models in [10,11]. Concerning the separation induced by gravity, following the decomposition of particle velocity into local fluid velocity and Stokes velocity, the source term S_i for the transport equation is:

$$S_i = div(\alpha_l \boldsymbol{u}_s N_i) \qquad (4)$$

where u_s is the vertical Stokes velocity in the case of small inclusions whose particle Reynolds number is lower than 1.
A particular attention has been paid on inclusion entrapment at the liquid metal / slag interface. It is modeled following the approach based on a deposition law developed initially by Wood [15] and adapted to a free liquid surface condition by Xayasenh [16]. The entrapment of inclusions at the ladle walls is not considered.

Concerning the aluminum stirred reactor, the axisymmetric feature allows us to develop a 2D homemade code to solve the equation 2. On the contrary, since the flow in the steel ladle is 3D in nature (due to the location of the porous plugs), the equation 2 is solved within the frame of the CFD code FLUENT.

Numerical simulation of the Al flotation tank

A cylindrical laboratory scale apparatus with an inner diameter of 33 cm and containing 70 kg of molten aluminum at 1000 K was modeled (figure 2). At the tip of each blade, a gas injector blows a mixture of argon and chlorine into the melt. Bubble size was calculated with correlations established from water experiments and transposed to liquid aluminum by Waz [17].

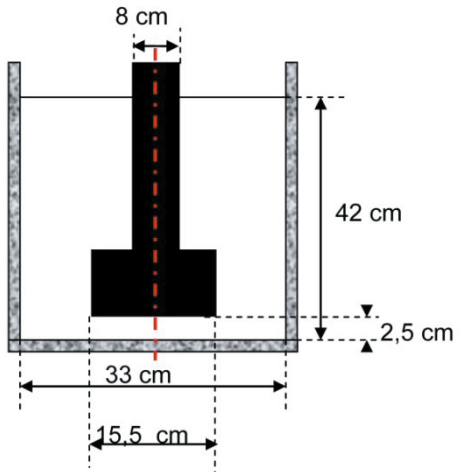

Figure 2: Schematic representation of the laboratory scale apparatus

In an industrial cast house, tuning of the flotation process is achieved with three parameters that are gas flow rate, rotor speed and location of the rotor in the tank. Dimensions of the pilot tank being relatively small, the rotor is positioned closed to the bottom in order to allow significant residence time of the bubbles into the melt. Influence of the gas flow rate and rotor speed on the process efficiency is studied through three different cases, referenced in table I.

Table I: Operating conditions

	N (RPM)	Q_g (Nm^3/h)
A	250	0.5
B	250	1.5
C	500	0.5

In the following calculations, we consider alumina inclusions with a 3900 $kg.m^{-3}$ density. Initial size distribution of the inclusions was established using the mean of several measurements performed with a Liquid Metal Cleanliness Analyzer (LIMCA^{TM}). Twenty-three classes of inclusions were considered with representative diameters spanning from 2.5 µm to 205 µm. As the resolution of LIMCA^{TM} does not go below 20 µm, the measured distribution was extrapolated (the four smallest classes) to obtain a more realistic distribution. The complete distribution is reported in figure 3 and is used as the initial PSD (Particle Size Distribution).

At time t=0, the inclusions spatial distribution is supposed to be homogeneous in the melt.

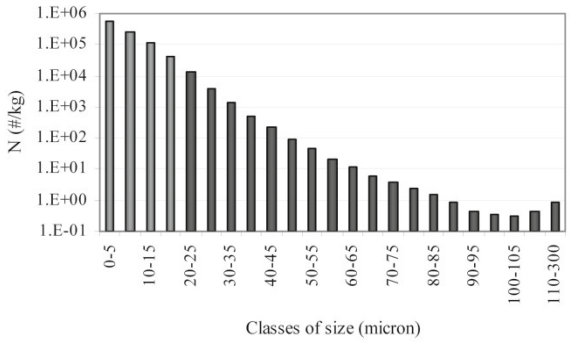

Figure 3: Initial PSD. In gray, the extrapolated part of the distribution

Fluid flow and bubble repartition

CFD calculations show a relatively weak influence of the dispersed gas phase on the liquid metal flow pattern in the bulk of the reactor. Figure 4 gives the calculated time-averaged streamlines in the steady state for case B. A weak swirl is noticed near the shaft, close to the surface of the bath. It becomes more pronounced at higher rotation speed. Turbulence properties (ε and k) reach their maximum value around the blades of the rotor where the shear is strong.
As shown in figure 5, increasing rotor speed with a constant gas flow rate improves bubbles dispersion in the reactor, leading to an upward trend in mean gas holdup. No significant difference between bubbles dispersion in cases A and B (same rotor speed and higher flow rate) is noticed.
On the other hand, the highest mean gas holdup is predicted for case B, which has a gas flow rate 3 times higher than cases A and C. Average residence time of the bubble into the melt ranges from 0.6 to 0.86 depending on the case considered.

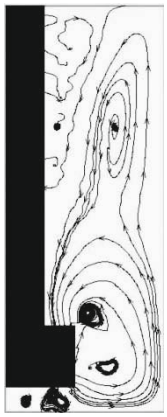

Figure 4: Computed streamlines for case B

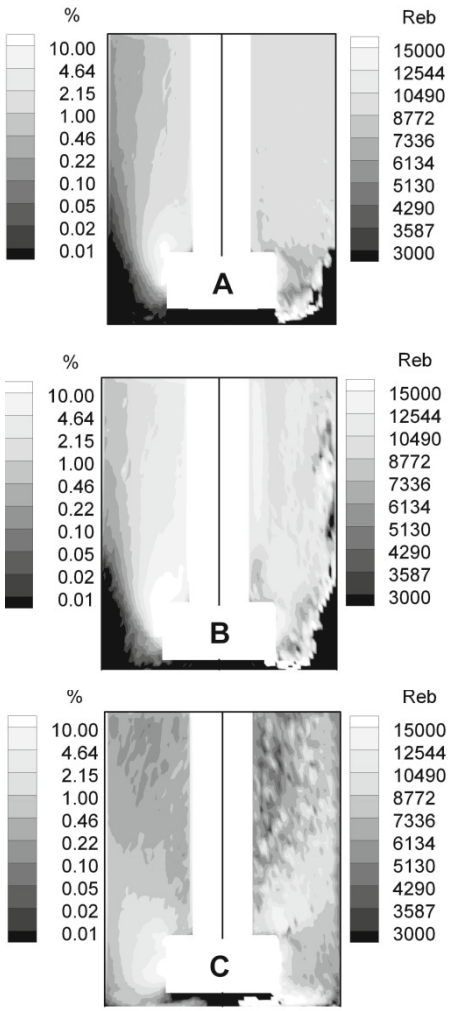

Figure 5: Computed local gas holdup (volume fraction in %) and bubbles Reynolds number for cases A, B and C

Time evolution of the inclusion population

A ten minute treatment was simulated for the three cases studied. Time evolution of the total number of inclusions into the melt is reported in figure 6. After a strong decrease in the total number of inclusions at the beginning of the treatment, the rate of removal slowly softens. This change is due only to the depletion of the number of inclusions in the melt (driving force of agglomeration and flotation phenomena).

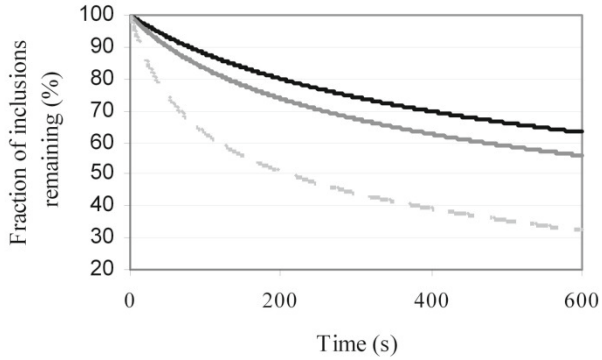

Figure 6: Computed evolution of the total number of inclusions into the melt for case A (black), B (gray) and C (doted gray).

Cases A and B have the same rotor speed, but the gas flow rate of case B is three times higher than that of case A. It appears that cases A and B are relatively close to each other, case B being slightly more efficient. Case C has a low gas flow rate (equivalent to case A) but a high rotor speed. As previously seen, those operating parameters allow a good dispersion of the bubbles into the liquid bath and especially in the zones of high turbulence intensity, which is the best situation to promote flotation.

Agglomeration versus flotation

For comparison purposes we have plotted in figure 7, the flotation removal rate (the negative sign of the rate is not mentioned on the figure) and the evolution rate due to agglomeration for the same class of inclusions. Inclusions considered on this plot have a representative diameter of 47.5 µm and the operating conditions correspond to case A. The plotted values are computed at the beginning of the treatment (initial time).
Under those conditions the computed evolution rate due to agglomeration is positive in the whole tank, which means that the birth rate is greater than the death rate.
Comparison between the left and right parts of figure 7 reveals that, in a large part of the tank, removal by flotation is in the same order of magnitude as birth by agglomeration. This means that equilibrium between agglomeration and flotation may be reached locally for certain classes of inclusions, which results in very low evolution rates.

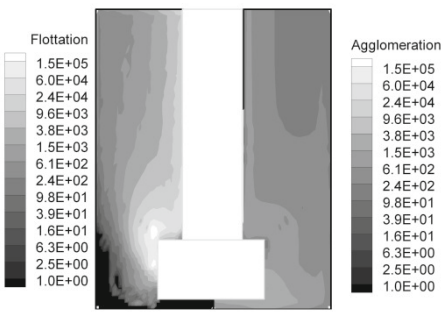

Figure 7: Computed flotation removal rate (left) and agglomeration feed rate (right) ($m^{-3}.s^{-1}$)

PSD after 5 and 10 minutes of treatment are shown for case B in figure 8. No significant difference between those two PSD can be observed, except for the smallest classes that keep on loosing inclusions.
At the beginning of the treatment coarser inclusions (d_p > 70 µm) are quickly removed from the melt since they are more likely to collide with bubbles, and because of their high settling rate. Evolution rates (agglomeration, flotation and settling) of the smallest classes remain quasi constant with respect to time since the probability of collision and flotation are very low. Intermediate classes (40 < d_p < 70 µm) reach a balance between removal by flotation and feed by agglomeration, as previously explained.

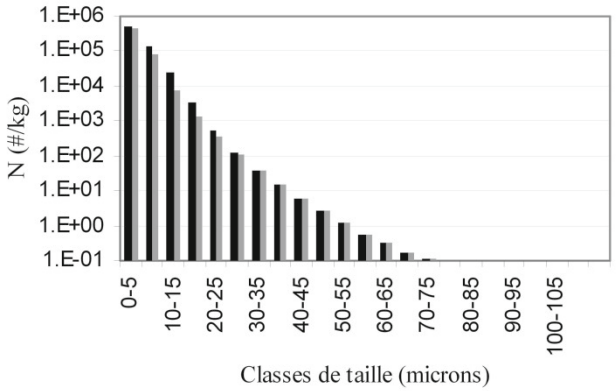

Figure 8: PSD after 300 sec. (black) and 600 sec (gray), for case B

Numerical simulation of the steel gas stirred ladle

The numerical simulation is applied to a full scale 60 t steel ladle. Argon is injected through two porous plugs, located at the base of the ladle, into a bath of molten steel contained in a slightly tapered cylindrical vessel. Argon flow rate used for modeling is small (less than 30 Nl/min for each plug), a relatively low flow rate for such a quantity of liquid steel. The model assumes a uniform liquid temperature equal to 1600 °C.

Fluid flow and bubble repartition

Two-phases (liquid/bubbles) flow is calculated by the CFD commercial code Fluent and the liquid steel velocity and argon plume region on a plane passing through the porous plugs of the ladle are shown in Figure 9. One can observe the shapes of the two bubble plumes rising from the two porous plugs (the isosurface of gas volume fraction equal to 1% is drawn). These regions are characterized by weak bath aeration as the distance from the porous plug increases. The gas volume fraction was found to be below 5% in each plume. The liquid metal flow is associated with two recirculation zones in each half of the plane of symmetry. Turbulence is strongly non-uniform and the dissipation rate of the turbulence kinetic energy ranges between 10^{-6} and 10^{-1} m^2 s^{-3}.

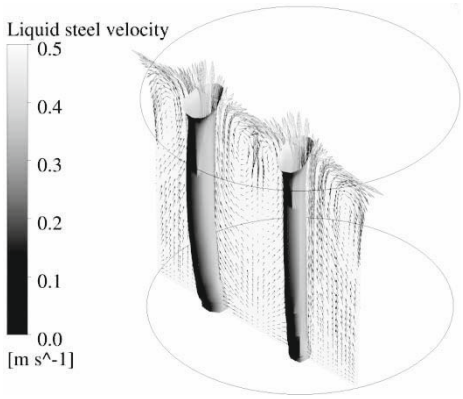

Figure 9: Predicted velocity of the liquid steel along with the argon plumes (isosurface of the 1% gas volume fraction) in a vertical plane passing through the porous plugs.

Time evolution of the inclusion population

With the aim of highlighting the capability of such numerical model to predict the time evolution of an inclusion population, a typical initial distribution of inclusions is considered in the 60 t stirred ladle for the hydrodynamics condition simulated above. For confidential reasons, the initial distribution does not correspond to real industrial conditions but is sufficiently close so as to the conclusions might be significant.

The inclusion population is discretized into twenty different size classes in the range [1-200 µm]. Figure 10 compares the PSD after 100 s of gas stirring (blue) with the one obtained at the end of the 600 s of treatment (red). The computed distribution continuously evolves with time, as larger size particles appear due to the agglomeration of small size particles leading to an increase of the Sauter diameter d_{32} (diameter of a sphere that has the same volume/surface area ratio as the inclusion of interest) over time as shown (see figure 11). Since the flotation and sedimentation mechanisms are strongly dependant of the particle size, the large size aggregates are preferentially removed. As a consequence the total mass of inclusions in the ladle diminishes and the associated rate of removal is not constant but slowly increases.

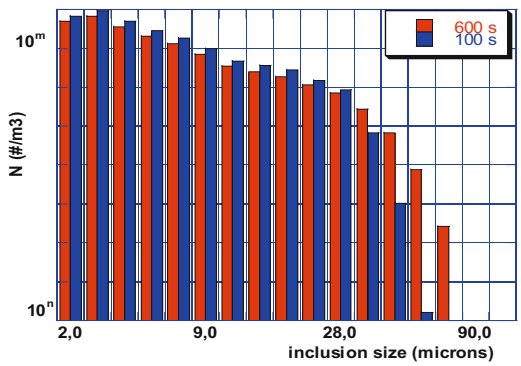

Figure 10: PSD after 100 and 600 seconds (arbitrary Y-coordinate).

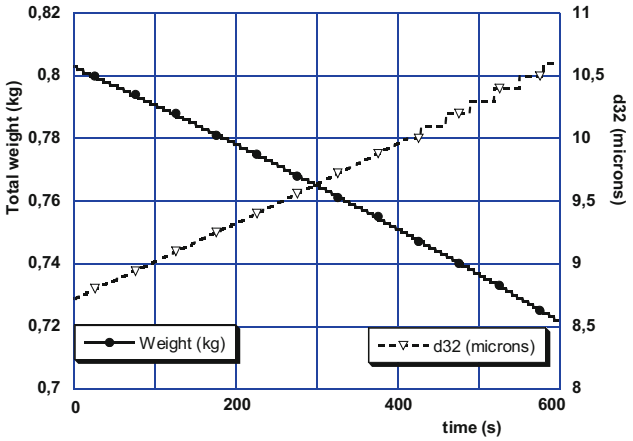

Figure 11: Total mass of the inclusion population and Sauter diameter of the PSD versus time

The numerical simulation allows us to compare the relative importance of the different removal mechanisms on the inclusion population. The frequencies of the aggregation, flotation, settling and capture on the free surface mechanisms have been reported in figure 12 (at the beginning of the process i.e. at time equal to 30 s). The sign (-) or (+) indicates that the numerical density of a given class decreases or increases following either the aggregation, flotation, separation and entrapment processes. As an example, the aggregation frequency F_A is calculated as:

$$F_A = \int_V (B_i - D_i) dV \qquad (5)$$

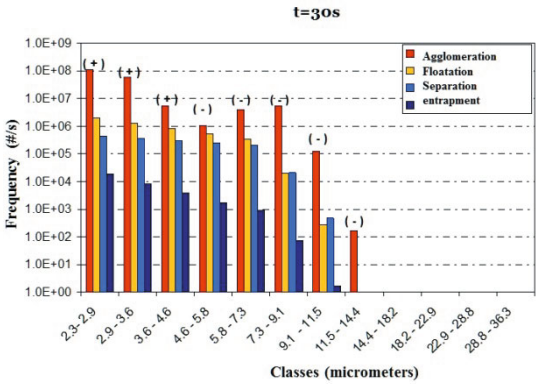

Figure 12: Frequency of mechanisms as a function of inclusion size at 30 s – (-): reduced (+): produced

The figure 12 clearly highlights that the major role is played by agglomeration, since the frequency of the flotation mechanism is two orders of magnitude lower than the agglomeration one. This is the main reason why the PSD continuously evolves with time and does not reach the equilibrium in this example (as was noticed in the case of Al). Large size inclusions are produced by agglomeration with a rate larger than the flotation removal rate.

This strong difference between Al and steel reactors stems from the blowing rate which can be much stronger in Al making. The efficiency of the flotation mechanism is then directly influenced by the gas holdup and by the dispersion of the bubbles into the bath. The turbine blades allow a large dispersion of the bubbles within the Al reactor whereas the bubble swarms are weakly dispersed in the gas stirred ladle.

Conclusion

Nowadays the numerical modelling affords the possibility to simulate complex three-phase metallurgical reactor by combining CFD and Population Balance resolution. Hence a mathematical model of inclusion behaviour in a stirred ladle has been built up step by step. First the turbulent flow is simulated using the Euler-Euler method, taking into account all the interaction forces between the two phases (gas bubbles and liquid steel). Second the numerical model handles both agglomeration and removal mechanisms (flotation, gravity separation, free surface entrapment) together with the convective transport of inclusions into the melt. The coupling of convective transport equation and the PBE is achieved using a time-splitting technique. The discrete class method with the cell average feature was adopted to solve the PBE and was implemented into CFD codes.
As an illustration, the numerical modeling is applied to both an Al laboratory reactor and an industrial steel ladle. The results emphasize the relative role of agglomeration versus flotation as a function of the blowing rate and of the dispersion of bubbles into the bath.

Acknowledgement

This study was a part of the CIREM project (inclusion behaviour in the metallurgical reactors) supported by the French National Research Agency (ANR06 MATPRO 0005).

References

[1]Nakanishi K., Szekely J., "Deoxidation kinetics in a turbulent-flow field", *Transaction of the Iron and steel institute of Japan*, Vol. 15, 10 (1975), 522-530

[2] Sahai Y., Guthrie R.I.L., "Hydrodynamics of gas stirred melts 1. Gas liquid coupling", *Met. Trans B*, Vol. 13 , 2, (1982), 193-202

[3] Sahai Y., Guthrie R.I.L., "Hydrodynamics of gas stirred melts 2. Axisymmetrric flows", *Met. Trans B*, Vol. 13 , 2, (1982), 203-211

[4] Hallberg M., Jönsson P.G., Jonsson T.L.I., Erikson R., *Scandinavian Journal of Metallurgy*, (2005), Vol. 34, 41-56

[5] Aoki J., Thomas B. G., Peter J., Peaslee K. D., Proc. of Iron and Steel Technology Conference AISTech, 2004, 1045

[6] Söder M., Jönsson O., Jonsson L., Nzotta M., *Steel Research Int.*, (2005), 481

[7] Gardin P., Gauthier S., Simonnet M., "Multiphase Model for Predicting the Elimination of Inclusions inside a Liquid-Steel Ladle", *Advanced Engineering Materials*, (2011), Vol.13, 538-542

[8] Kwon Y.-J., Zhang J., Lee H.-G., "A CFD-based Nucleation-growth-removal Model for Inclusion", *ISIJ International*, (2008), 48, 7-14.

[9] Claudotte L., Rimbert N., Gardin P., Simonnet M., Lehmann J., Oesterle B., "A Multi-QMOM Framework to Describe Multi-Component Agglomerates in Liquid Steel", *AICHE Journal*, (2010), Vol. 56, 2347-2355

[10] Daoud I. L. A. , Rimbert N., Jardy A., Oesterle B., Hans S., Bellot J.P., "3D modelling of the aggregation of oxides inclusions in a liquid steel ladle: two numerical approaches", *Advanced Engineering Materials*, (2011), Vol.13, 543-549

[11] Mirgaux O., Ablitzer D., Waz E., Bellot J.P., "Mathematical modelling and computer simulation of molten aluminium purification by flotation in stirred reactor", *Met Trans B*, Vol. 40B, (2009), 363-375.

[12] Kumar S., Ramkrishna D., *Chem. Eng. Sci*., (1996), Vol.51, 1311-1332.

[13] Toro E.F., *Riemann solver and numerical methods for fluid dynamics: a pratical introduction*, (Springer, Berlin, 1999).

[14] Kumar J., Peglow M., Warnecke G., Heinrich S., Mörl L., Chem. Eng. Sci., 2006, vol.61, 3327-3342

[15] Wood N.B., *Journal of Aerosol Science*, (1981), Vol.12, 275

[16] Xayasenh A., Duval H., Joly L., "Analyse qualitative du transport turbulent d'inclusions à l'interface métal liquide/laitier" (Proc. of the Symposium Matériaux, Nantes, France, edited by the Materials French Society on CD-ROM, 2010)

[17] Waz E., Carré J., Le Brun P., Jardy A., Xuereb C. and Ablitzer D., "Physical modeling of the aluminum degassing process: Experimental and mathematical approaches", *Light Metals. TMS*, (2003), 901-907